Energy Proceedings
8, 2022

Preliminary Design and Thermodynamic Analysis of a Novel Water-Electricity Cogeneration System#

Tingyu Xiao, Chao Liu*
Key laboratory of low-grade Energy Utilization Technologies and Systems, Ministry of Education, School of Energy and Power Engineering, Chongqing University, Chongqing 400030, China

ABSTRACT

By combing a supercritical CO_2 (sCO_2) Brayton cycle and a direct contact membrane distillation (DCMD) block, an energy-efficient water and electricity cogeneration is proposed. Two layouts of the hybrid system are designed. Thermodynamic analysis for the hybrid system is carried out by considering the effects of the operation conditions and the membrane properties. With the on-design parameters input, the energy efficiency of the layout 1 and layout 2 is 38.48% and 37.52%, respectively. By optimizing the parameters, the energy efficiency can be further improved. Although the layout 1 has higher energy efficiency, the layout 2 has larger variation ranges of the parameters due to the less limitation of the pinch point temperature difference in the intermediate heat exchanger (IHX).

Keywords: sCO_2 power cycle, Membrane distillation, Electricity/water cogeneration, Thermodynamic analysis

1. INTRODUCTION

Desalination technologies become one of the practical solutions to meet the increasing demand of fresh water. However, the desalination processes are often energy intensive, consuming large amounts of electrical energy or high-temperature heat, which makes the desalination technologies always costly[1]. Power and water cogeneration can use the thermal energy or electricity of the power plant to drive the desalination process, so as to realize energy efficient utilization and reduce the cost of seawater desalination[2, 3].

Compared with the conventional steam Rankine cycle, sCO_2 Brayton cycle benefits attractive efficiency, compactness, capital cost reduction, clean and inexpensive working fluid. sCO_2 Brayton cycle is expected to be the next generation of power cycles for nuclear reactors and solar thermal power plant, waste heat recovery and fossil energy (operating at 500 ℃ - 900℃)[4]. With a turbine inlet temperature of 550 ℃, the thermal efficiency of sCO2 cycle can reach 45.3%, which is similar to the thermal efficiency of the helium Brayton cycle at a maximum temperature of 850 ℃ [5]. Despite the high efficiency, there is a larger amount of waste heat (about 50% of the input energy) rejected to the heat sink in the sCO_2 power cycle [6]. Many studies are devoted to utilize this water heat in different forms to improve the overall efficiency. Wang et al. [7] compared the utilization of organic Rankine cycles and transcritical CO_2 cycle for recovering this waste heat for power generation. Yuan et al. [8] proposed the integration of sCO_2 power cycle with an ejector transcritical CO_2 refrigeration cycle to combine cooling and power. Tang et al. [9] proposed a combination of sCO2 Brayton cycle and an absorption heat transformer to upgrade the energy level of the waste heat in the sCO_2 power cycle. However, there are few studies about the water and electricity cogeneration based on the sCO2 power cycle.

Membrane distillation (MD) is a potentially promising desalination technology, which combines the membrane desalination and thermal desalination [1]. MD can be divided into four types: DCMD, air gap membrane distillation, sweeping gas membrane distillation and vacuum membrane distillation. Among them, the DCMD has relatively simple configuration, which is the earliest and most widely studied MD technology[10]. Although MD typically has higher energy consumption than other separation techniques, the high salt rejection, the ability to treat high-salinity feed waters and couple with renewable energy or waste energy makes it very attractive and profitable [11-13]. The temperature of the exhaust sCO_2 flow matches the heat source temperature of MD. Coincidentally, the cool feed sea water in MD could serve as the cooling agent of sCO_2. However, so far, few researches have studied the performance of a hybrid system composed of a sCO_2 power cycle and MD, which will be attractive for the electricity and clean water cogeneration.

To fill the research gap, this work proposes a new system consisting of a sCO_2 Brayton cycle and a DCMD. The DCMD is used to harvest the thermal energy rejected by sCO2 power cycle, leading to an improvement in the energy conversion efficiency of hybrid system. Two layouts are designed. Thermodynamic performance of the two layouts are studied and compared.

2. THE SCO_2-MD HYBRID SYSTEM

2.1 System description

The electricity and water cogeneration system is combined by a simple sCO_2 power cycle and a DCMD desalination block. Two layouts of the cogeneration system are shown in Fig.1.

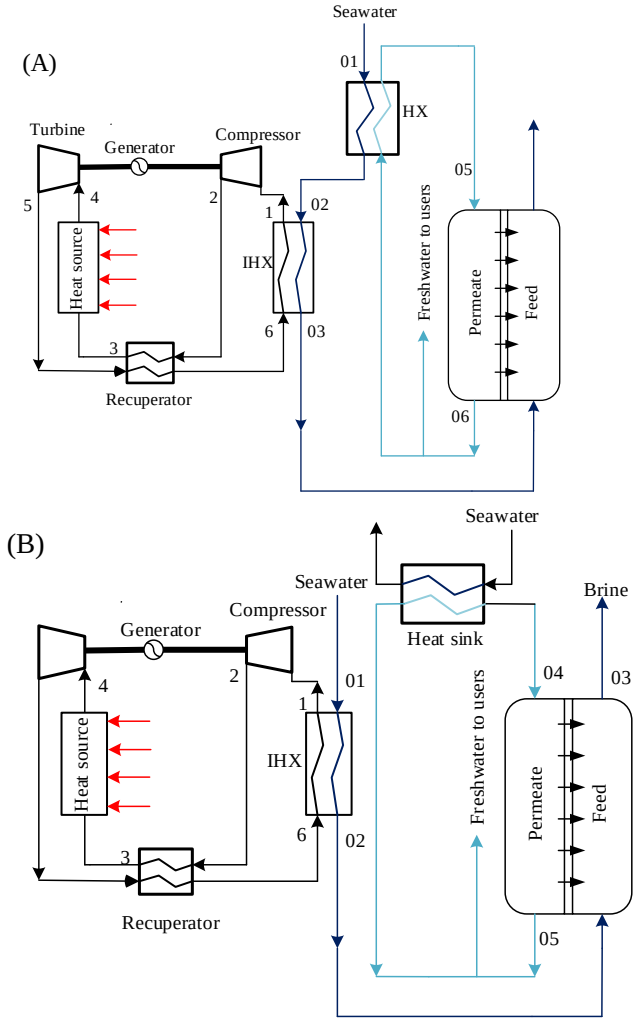

Fig.1 Schematic diagram of the hybrid system (a. Layout 1; b. Layout 2)

In layout 2, the cold seawater directly enters the IHX and is heated by the exhaust sCO_2 flow from the recuperator, while sCO_2 flow is cooled by the sea water introduced into DCMD. In DCMD, a microporous hydrophobic membrane is used to separate the feed side (hot seawater or high salinity wastewater heated in IHX) and the permeate side (cool freshwater). The temperature difference between the two sides generated the difference in partial vapor pressure at the membrane-liquid interfaces, which drives a vapor flux against the concentration gradient across the membrane, combined with the nearly 100% rejection of salt. The vapor flux condenses upon contact with the fresh water flow at the permeate side. Meanwhile, the heat is transferred across the membrane in the form of latent heat of vaporization and conduction. At permeate side exit, the heated freshwater is divided into two streams. One stream is provided to the users to satisfy the demand of water, of which the mass flow is equal to the total transmembrane water flux. At the same time, the other stream enters the heat sink to be cooled down to the design temperature by the cold sea water and recycles.

Different from layout 2, there is a heat exchanger (HX) for heat recovery in layout 1. In the HX, the cold sea water introduced to the DCMD is preheated by the warm fresh flow from the permeate side.

2.2 Thermodynamic model construction

Both sCO_2 power cycle and DCMD have mature mathematical models, which have been discussed deeply in the previous literatures [4, 5, 14-16]. The combined cogeneration cycle will be modeled based on the energy balance of individual components.

In simple sCO_2 Brayton cycle, thermodynamic relation for the recuperator is given by:

$$h_5 - h_6 = h_3 - h_2 \quad (1)$$

$$\varepsilon = (T_5 - T_6)/(T_5 - T_2) \quad (2)$$

The sCO_2 flow in the system is estimated as function of the heat input and the enthalpy rise in the reactor:

$$m_{co_2} = \frac{\dot{Q}_{core}}{(h_4 - h_3)} \quad (3)$$

The power production and consumption in turbomachinery devices can be estimated by:

$$\dot{W}_T = \dot{m}_{co_2}\eta_T(h_4 - h_{5s}) \quad (4)$$

$$\dot{W}_C = \dot{m}_{co_2}(h_2 - h_1)/\eta_C \quad (5)$$

Fig.2 shows the schematic diagram of heat and mass transport across the membrane. As the heat transfer across the membrane creates thermal boundary layers on both sides, the temperatures at the membrane surfaces are different from the bulk temperatures, in a phenomenon known as temperature polarization[17].

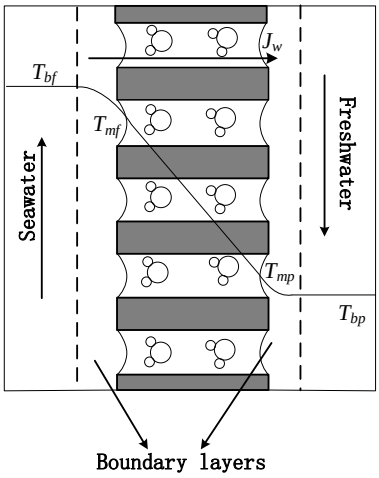

Fig.2 Schematic diagram of heat and mass transport across the membrane

The temperature polarization and the high hydraulic pressure of permeate flow could decrease the vapor flux, J_w. Therefore, J_w is a function of the vapor pressure difference between the membrane surfaces, which is affected by the transmembrane temperature difference, hydraulic pressure difference and concentration difference and can be described as flowing:

$$J_w = B_w[P_v(T_{mf}, S_f) - P_v(T_{mp}, 0)] \quad (6)$$

Where B_w (kg m^{-2} s^{-1} Pa^{-1}) is the membrane permeability coefficient, which is determined by the pore size, tortuosity, porosity and thickness of the membrane [10]. P_v (Pa) is the vapor pressure; T_{mf} and T_{mp} (℃) are the temperatures at the interface on the feed and permeate side of the membrane, respectively; P_h(Pa) is the hydraulic pressure. For the successful operation, the vapor difference induced by the temperature difference should be a higher degree than the opposing ones induced by salinity difference and hydraulic pressure difference.

The relationship between P_v and the temperature T is described by the Antoine equation [18]:

$$P_v = \exp(23.328 - \frac{3841}{T-45}) \quad (7)$$

An increment in salinity decreases the equilibrium vapor pressure of solution, which is in agreement with Raoult's law given by[19]:

$$P_v = (1-S)P_{v,s=0} \quad (8)$$

As water is transported through the membrane, heat will also be carried across. The heat flux is the sum of the latent heat of vaporization transfer across the membrane and the heat transferred across the membrane by conduction, which can be described by:

$$q_m = J_w H_{vap} + \frac{K_m}{\delta}(T_{mf} - T_{mp}) \quad (9)$$

where H_{vap} (J kg^{-1}) is specific enthalpy of vaporization, (W m^{-1} K^{-1}) is the thermal conductivity of the membrane, δ (m) is the membrane thickness. K_m can be estimated from the thermal conductivity of the gas trapped within the pores, the polymer material, and the porosity[20]. It can be concluded that convective heat transfer is necessary for operation of the system, while conductive heat transfer represents an energetic loss.

The relationship between the temperature at the membrane surface and the bulk temperature can be described by:

$$T_{mf} = T_{bf} - \frac{q_f}{h_f} \quad (10)$$

$$T_{mp} = T_{bp} + \frac{q_p}{h_p} \quad (11)$$

where q_f and q_p (W) are the convective heat flux across the boundary layer, h (W m^{-2} K^{-1}) is the convective heat transfer coefficient.

The overall heat transfer across the membrane with the steady state condition can be written as Eq. (12). J_w and q of every single section can be calculated by this balance.

$$q = q_f = q_p = q_m \quad (12)$$

where $\dot{D}$ is the total produced freshwater (kg/s), h_{ref} is the distillate specific reference enthalpy (J/kg).

The energy efficiency of the cogeneration system is defined as the percentage of the effective energy utilization in the total energy input:

$$\eta_{system} = \frac{\dot{W}_T - \dot{W}_C - \dot{W}_{pump} + J_w H_{vap}}{\dot{Q}_{core}} \quad (13)$$

The assumption condition in key components and input parameters used in the analysis are given in Table 1. t_{fi} and t_{pi} represents the inlet temperature of the feed side and permeate side in the membrane module, respectively. A_{nor} is the normalized membrane area, which is defined as the membrane area divided by the feed flow rate. It should be noted that the variation range of the parameter is limited considering the pinch point problem in the IHX.

Table 1. Initial parameters of the hybrid system

Parameters	Value
t_0, t_{sea} (℃)	20
P_0 (MPa)	0.1013
P_{max} (MPa)	20
P_1 (MPa)	7.4
t_1 (℃)	32
t_{max} (℃)	550
$\triangle t_E$ (℃)	3-20

t_{fi} (℃)	60
t_{pi} (℃)	25
A_{nor} (m^2 s kg^{-1})	0.5
B_w (kg m^{-2} s^{-1})	1e-6
K_m (W m^{-1} K^{-1})	0.04
Thickness (μm)	100
$\dot{Q}_{core}$ (MW)	500

3. RESULT AND DISCUSSION

3.1 Model validation

There is no experimental research on the proposed hybrid system so far, thus sCO_2 power cycle and DCMD are validated individually. The present sCO_2 power cycle model will be validated by the available calculated data in literatures [21]. The comparison results are listed in Table 2. The relative error is almost equal to 0. It can be concluded that the sCO_2 power cycle is simulated in a reliable way. DCMD model is validated by those experimental data of DCMD system reported in the literature[22]. In the DCMD experiment, a PTFE membrane with no support layer was used. Feed flow and permeate flow were in counter-current flow mode with a flow rate of 1.1L/min. The feed liquid was 35g/L NaCl solution. The membranes had a thickness of 67 μm. The module channel had a length of 146 mm, a width of 95 mm, a depth of 0.787 mm, and a total active membrane area of 138.7 cm^2. The water flux measured with various temperature couples in experiment and the simulation results with the same conditions are compared, as listed in Table 3. It can be seen that there is a good agreement between the simulation results and the experimental results, with a maximum relative error of 8.5%.

Table 2 Validation of simple sCO_2 power cycle

Parameter[a]	Present work			Reference data [21]		
t_{min} (℃)	W_T (MW)	W_{net} (MW)	η_{th} (%)	W_T (MW)	W_{net} (MW)	η_{th} (%)
32	25.60	21.22	37.9	25.62	21.26	38.2
42	33.65	21.53	36.06	33.26	21.14	35.67

[a] η_T=0.914, η_C=0.9, ε_{Recp}=0.991, tmax=550 ℃, P_{max}=20 MPa

Table 3 Validation of DCMD desalination block

Parameters		Present work	Reference data [22]
t_p (℃)	t_f (℃)	Water flux (kg/(s·m^2))	Water flux (kg/(s·m^2))
20	40	0.002	0.002
30	44	0.0017	0.0018
30	53	0.0034	0.0035
31	57	0.0043	0.0047

3.2 The system on-design evaluation

Under the steady-state simulation, the thermodynamic performances of the two layouts are investigated and summarized in Table 4. With the same input parameters, the net output power and thermal efficiency of the power blocks of the two layouts are equal. However, in Layout 1, more seawater flow is required to cool the sCO_2 flow due to the higher temperature of seawater induced into the IHX, which leads to a larger production of freshwater, and a larger consumption of the pumping power. Therefore, the overall net output power of the layout 1 is slightly smaller than that of the Layout 2. The overall energy efficiency of Layout 1 is about 1% higher than that of the Layout 2.

Table 4. The on-design thermodynamic performance of the hybrid system

Parameters	Value	
	Layout 1	Layout 2
$W_{net,PB}$ (MW)	154.50	154.50
η_{PB} (%)	30.90	30.90
Qcapacity(m^3/day)	1411.45	1023.52
η_{DB} (%)	38.48	37.52
$W_{net,system}$ (kW)	154.36	154.38
η_{system} (%)	38.48	37.52

3.3 Parameter analysis of the hybrid system

A parametric analysis is conducted to study the effects of important parameters on the thermodynamic performance of the combined cogeneration system. The total energy efficiency of the hybrid system (η_{system}) is selected to evaluate the overall thermodynamic performance of the electricity and water cogeneration system. According to Eq. (13), η_{system} depends on the overall net power output and the freshwater production with a fixed heat input.

Fig.3 shows the effects of the turbine inlet temperature on the total energy efficiency of the hybrid system. According to the applicable temperature range of the sCO_2 Brayton cycle and the temperature that can be reached by the nuclear reactor, solar collector and fossil fuel boiler, t_4 is set as 550-750 ℃. With the increase of t_4, the output power of the sCO_2 power block increases, which leads to the increase of the total net power output. On the other hand, the mass flow rate of CO_2 decreases with t_4, so mass flow rate of the cooling seawater and the freshwater production decrease. Since η_{system} is dominated by the total net power output, η_{system} increases with t_4. When t_4 increases from 550 ℃ to 750 ℃, the energy efficiency of layout 1 increases by

about 15%, while the energy efficiency of layout 2 increases by about 11%. The energy efficiency of the layout 1 keeps about 1% higher than that of layout 2.

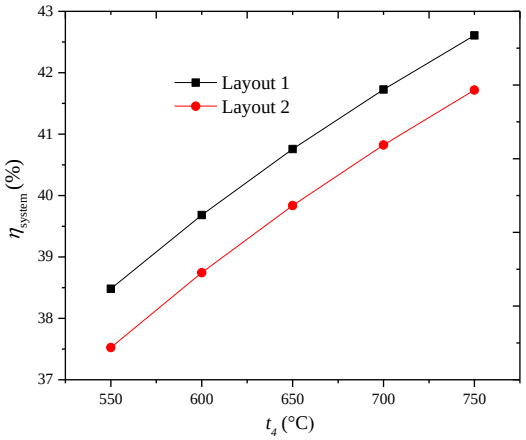

Fig.3. Total energy efficiency of the hybrid system with varied turbine inlet temperature

The variation of operating conditions in DCMD system and membrane properties only affects the performance of the desalination blocks, but not the power production of the sCO_2 power cycle. Fig. 4 shows the effects of t_{fi} and normalized membrane area on η_{system}. The transmembrane water flux increases with t_{fi} and the normalized membrane area. Therefore, η_{system} increases with t_{fi} and normalized membrane area. In general, the energy efficiency of the layout 1 is higher than that of the layout 2 with the same input parameters. However, due to the limitation of the pinch point temperature difference between in IHX, the variation ranges of parameters in the layout 1 will be smaller. The set value of t_{fi} in the layout 1 can hardly reach 70℃, and the set value of A_{nor} is also difficult to reach 2 m^2 s kg^{-1}. Therefore, in the layout 2, when t_{fi} is higher than 70℃ or A_{nor} is larger than 2 m^2 s kg^{-1}, the energy efficiency can exceed that of the layout 1.

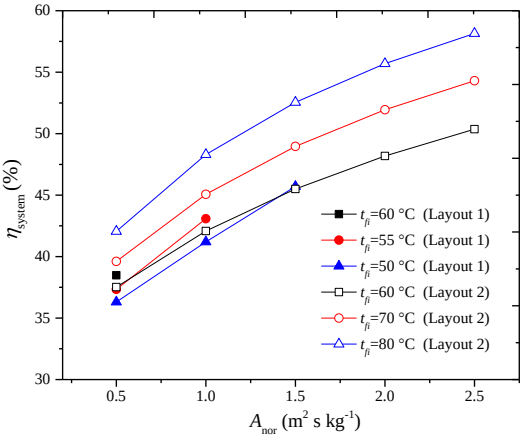

Fig.4 Total energy efficiency of the hybrid system with varied t_{fi} and A_{nor}

The permeability coefficient and the thermal conductivity are two main properties of the membrane. Fig. 5 shows the effects of B_w and K_m on η_{system}. With the increase of B_w, η_{system} increases because of the increment of the transmembrane water flux. With the increase of K_m, the water flux will decrease slightly, so the system energy efficiency will decrease slightly. With the increase of B_w and K_m, the difference between the energy efficiency of the layout 1 and the layout 2 increases, and the maximum difference is 1.4%.

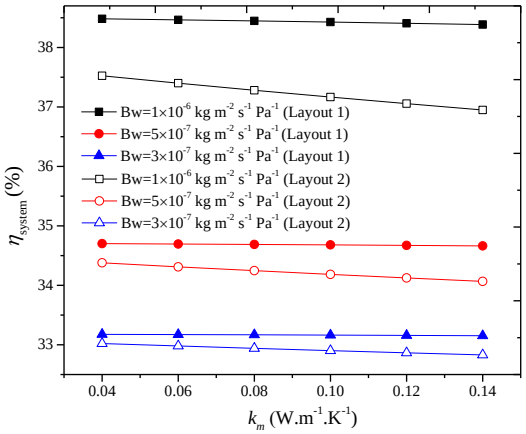

Fig.5 Total energy efficiency of the hybrid system with varied membrane properties

4. CONCLUSIONS

In this work, a new electricity and freshwater cogeneration system based on sCO_2 power cycle and DCMD desalination technology is proposed, aiming at an energy-efficient scheme for large-scale water and power supply. Two layouts of the hybrid system are proposed. Thermodynamic analysis of the hybrid system is implemented under the steady-operation condition, and the main research findings can be outlined as follows:

(1) With the on-design parameters input, the net power output and the fresh water production of the layout 1 are 154.36 MW and 1411.45 m^3/day, respectively. The net power output and the freshwater production of the layout 2 are 154.38 MW and 1023.52 m^3/day, respectively. The energy efficiency of the layout 1 and layout 2 is 38.48% and 37.52%, respectively.

(2) The energy efficiency of the hybrid system can be improved by increasing the turbine inlet temperature, the feed seawater temperature, the normalized membrane area, and the permeability coefficient of the membrane, or decreasing the thermal conductivity of the membrane.

(3) In general, the energy efficiency of the layout 1 is higher than that of the layout 2 with the same input parameters. However, due to the limitation of the pinch

point temperature difference between in IHX, the variation ranges of parameters in the layout 1 will be smaller. In the layout 2, when t_{fi} is higher than 70℃ or *Anor* is larger than 2 m^2 s kg^{-1}, the energy efficiency can exceed that of the layout 1.

ACKNOWLEDGEMENT

This work is supported by the National Natural Science Foundation of China (No. 52076018).

REFERENCE

[1] Deshmukh A, Boo C, Karanikola V, Lin S, Straub AP, Tong T, et al. Membrane distillation at the water-energy nexus: limits, opportunities, and challenges. Energy & Environmental Science. 2018;11:1177-96.

[2] Megahed MM. Nuclear desalination: history and prospects Desalination. 2001;135:169–85.

[3] Khamis I. A global overview on nuclear desalination. Int J Nucl Desalin. 2009;3.

[4] Wang X, Li X, Li Q, Liu L, Liu C. Performance of a solar thermal power plant with direct air-cooled supercritical carbon dioxide Brayton cycle under off-design conditions. Applied Energy. 2020;261.

[5] Dostal V DM, Hejzlar P. A supercritical carbon dioxide cycle for next generation nuclear reactors: Massachusetts Institute of Technology; 2004.

[6] Sarkar J, Bhattacharyya S. Optimization of recompression S-CO2 power cycle with reheating. Energy Conversion and Management. 2009;50:1939-45.

[7] Wang X, Dai Y. Exergoeconomic analysis of utilizing the transcritical CO2 cycle and the ORC for a recompression supercritical CO2 cycle waste heat recovery: A comparative study. Applied Energy. 2016;170:193-207.

[8] Yuan J, Wu C, Xu X, Liu C. Proposal and thermoeconomic analysis of a novel combined cooling and power system using carbon dioxide as the working fluid. Energy Conversion and Management. 2021;227.

[9] Tang J, Zhang Q, Zhang Z, Li Q, Wu C, Wang X. Development and performance assessment of a novel combined power system integrating a supercritical carbon dioxide Brayton cycle with an absorption heat transformer. Energy Conversion and Management. 2022;251.

[10] Alkhudhiri A, Darwish N, Hilal N. Membrane distillation: A comprehensive review. Desalination. 2012;287:2-18.

[11] Al-Karaghouli A, Kazmerski LL. Energy consumption and water production cost of conventional and renewable-energy-powered desalination processes. Renewable and Sustainable Energy Reviews. 2013;24:343-56.

[12] González D, Amigo J, Suárez F. Membrane distillation: Perspectives for sustainable and improved desalination. Renewable and Sustainable Energy Reviews. 2017;80:238-59.

[13] Khayet M. Membranes and theoretical modeling of membrane distillation: a review. Adv Colloid Interface Sci. 2011;164:56-88.

[14] Floyd J, Alpy N, Moisseytsev A, Haubensack D, Rodriguez G, Sienicki J, et al. A numerical investigation of the sCO2 recompression cycle off-design behaviour, coupled to a sodium cooled fast reactor, for seasonal variation in the heat sink temperature. Nuclear Engineering and Design. 2013;260:78-92.

[15] Lin S, Yip NY, Elimelech M. Direct contact membrane distillation with heat recovery: Thermodynamic insights from module scale modeling. Journal of Membrane Science. 2014;453:498-515.

[16] Soomro MI, Kim W-S. Performance and economic investigations of solar power tower plant integrated with direct contact membrane distillation system. Energy Conversion and Management. 2018;174:626-38.

[17] L. Martínez-Díez MIV-G. Temperature and concentration polarization in membrane distillation of aqueous salt solutions. Journal of Membrane Science. 1999;156:265-73.

[18] Stull DR. Vapor Pressure of Pure Substances. Organic and Inorganic Compounds. Indengchem. 1947;39:517-40.

[19] Qtaishat MR BF. Desalination by solar powered membrane distillation systems. Desalination. 2013;308:186–97.

[20] Phattaranawik J JR, Fane A G . Heat transport and membrane distillation coefficients in direct contact membrane distillation Journal of Membrane Science. 2003;212:177-93.

[21] Gibbs JP. Power conversion system design for supercritical carbon dioxide cooled indirect cycle nuclear reactors 2008.

[22] Gustafson RD, Murphy JR, Achilli A. A stepwise model of direct contact membrane distillation for application to large-scale systems: Experimental results and model predictions. Desalination. 2016;378:14-27.